DOI: 10.1021/cg900782g

CRYSTAL GROWTH & DESIGN Article

2010, Vol. 10
1544–1551

Crystallization of Hematite (α-Fe_2O_3) under Alkaline Condition: The Effects of Pb

Hong P. Vu,* Samuel Shaw, Loredana Brinza, and Liane G. Benning

School of Earth and Environment, University of Leeds, LS2 9JT, U.K.

Received July 8, 2009; Revised Manuscript Received February 1, 2010

ABSTRACT: The transformation of ferrihydrite ($5Fe_2O_3 \cdot 9H_2O$) to hematite (α-Fe_2O_3) under alkaline condition in the presence and absence of lead was for the first time investigated using in situ, time-resolved synchrotron-based energy dispersive X-ray diffraction combined with off-line chemical characterization and imaging. The results showed that the crystallization of hematite occurred via a two-stage process with goethite (α-FeOOH) as an intermediate phase. The presence of lead enhanced the formation of hematite and reduced the induction times (~20−30%) but had little effect on the mechanism of the transformation reactions. The reaction rates for the two systems (with and without lead) ranged from 12 to 259 $\times 10^{-4}$ s^{-1} and 19 to 461 $\times 10^{-5}$ s^{-1} for the first and second stage, respectively. The activation energies of nucleation of the two systems were 16(±3) and 9(±2) kJ/mol, while the activation energies for crystallization ranged from 41(±7) to 77(±14) kJ/mol. During the hematite crystallization, the majority of the lead in the system was rapidly and irreversibly incorporated into the final hematite, while only minor amounts of lead were released back into solution.

Introduction

Iron(III) (oxyhydr)oxides (e.g., goethite, α-FeOOH and hematite, α-Fe_2O_3) phases are widespread in many natural and engineered environments.[1,2] In natural systems, they are key components in the global biogeochemical cycle of iron and are important in the storage and transport of iron in many living organisms (e.g., animals and plants).[1] Iron(III) (oxyhydr)oxides particles also have a large metal (e.g., Cr, Pb, and Zn) sorption capacity due to their high surface area and reactivity. These properties have been exploited in various remediation technologies (e.g., groundwater treatment[3,4]) and cause these phases to have a significant effect on the speciation of many trace metals in the natural systems (e.g., rivers). In particular, Pb has been shown to have a strong affinity to iron(III) (oxyhydr)oxide phases in natural sediments and engineered systems.[5−7]

Poorly ordered ferrihydrite ($5Fe_2O_3 \cdot 9H_2O$) is often the first phase to form when ferric iron precipitates from solution, but it is thermodynamically unstable and in aqueous solutions it will gradually transform to crystalline phases such as goethite and hematite.[1] During this transformation, Pb adsorbed to the ferrihydrite surface can become incorporated into the crystalline end product, remain adsorbed to the mineral surface, or be released back into solution.[8,9] Understanding the link between the speciation of Pb and the crystallization of iron (oxyhydr)oxide is key to developing quantitative models for how Pb is sequestered within these phases. The lack of such information prevents accurate predictions of the nature or fate of Pb in natural and engineered environments. For example, iron (oxyhydr)oxide colloidal particles are thought to be the main transport vector for Pb in some natural systems (e.g., rivers) due to the significant correlation between Fe and Pb concentrations in river sediments.[5] However, the mechanism by which they become incorporated into such iron (oxyhydr)oxide colloidal particles is unknown. Furthermore, radioactive isotopes of Pb (e.g., ^{210}Pb) are thought to be a long-term risk associated with the disposal of radioactive wastes in cementitious deep geological repositories (pH > 12) which will contain large quantities of corroding metallic iron.[10] Understanding the mechanisms by which Pb can become incorporated or released from iron bearing minerals is therefore also key to developing risk assessment models to quantify the hazards these isotopes pose to the environment surrounding such repositories.

Many studies have followed the formation and transformation of ferrihydrite under different chemical conditions.[11−18] From this plethora of studies, it has been well established that goethite and hematite form via two different mechanisms. Goethite crystallizes from ferrihydrite via dissolution−reprecipitation, while hematite forms via aggregation and internal structural rearrangement of ferrihydrite nanoparticles.[11,12] In addition, it is known that the ratio of hematite to goethite formed during such transformation reactions and the rate of ferrihydrite crystallization are primarily controlled by the solution pH and temperature. With increasing pH and temperature, the crystallization rate increases[17] and in general hematite is favored at near neutral pH and high temperatures while goethite formation is favored at high and low pH and lower temperatures.[11,17,19]

With respect to Pb, studies related to the fate of Pb during the crystallization of ferrihydrite have only been conducted at low temperatures (≤70 °C) and at near neutral pH.[8,9,20−22] The results from these studies revealed that only a relatively small proportion of the sorbed Pb (up to ~10%) can become incorporated during the transformation, while up to ~20% of the total Pb is released back into solution during the late stages of crystallization.[9,20,22] However, there is no quantitative information available on how the speciation of Pb changes during ferrihydrite crystallization and how these processes are linked to the crystallization mechanisms of the individual phases (e.g., hematite and goethite). Previous studies have not obtained quantitative information on the phases forming

*Corresponding author: e-mail: vuhong@see.leeds.ac.uk; phone: +44 1133437869; fax: +44 1133435259.

 Published on Web 03/01/2010

(goethite and/or hematite); therefore, it is difficult to determine the processes that control the amount and mechanism of Pb uptake during crystallization. The presence of Pb during ferrihydrite crystallization has been shown to favor the formation of hematite over other iron (oxyhdr)oxide phases (e.g., goethite). However, in most experimental studies no monomineralic end product was produced,[8,9,20,22] and a quantitative evaluation of the transformation mechanisms and rates is still lacking. In addition, in these studies the reaction products were a mixture of various proportions of goethite, hematite, ferrihydrite, and lepidocrocite, and thus this poses a challenge when trying to quantify the kinetics and mechanisms of crystallization of each individual phase. Finally, the aforementioned studies were carried out using ex situ analysis techniques which looked only at a few steps in the reaction progress and thus they could neither define the influence nor the fate of Pb during the transformation reactions.

Therefore, the aim of this study was to quantify the role and fate of Pb during the crystallization of ferrihydrite in order to obtain a mechanistic understanding of how Pb becomes incorporated or is released during the reaction and to evaluate how this is linked to the mechanism of hematite and goethite crystallization. We have examined these reactions at high pH and temperatures and also evaluated the effect of Pb on the kinetics and mechanisms of hematite formation. In contrast to previous studies, we have for the first time employed an integrated range of techniques that could follow all aspects of the process both in the solids and solution phases at a high temporal scale. We have used in situ, synchrotron-based energy dispersive X-ray diffraction (EDXRD) to follow the transformation reactions in a time-resolved manner and combined these results with the quantification of the Pb speciation, the changes in surface area and electron imaging techniques. This unique multimethod approach to study reactions has allowed a link between the key aspects of the crystallization process and the uptake and release of Pb to be established.

Experimental Methods

Ferrihydrite Preparation. Ferrihydrite was synthesized following the procedure of Cornell and Schwertmann.[1] Freshly prepared ferrihydrite slurries were stored at 4 °C prior to the experiments. For each batch of ferrihydrite, the dried weight was determined from the weight loss of a known amount of slurry (in triplicate) upon drying a known aliquot at 50 °C for 24 h.

Adsorption and Transformation Experiments. Pb sorbed ferrihydrite (+Pb system) was produced by mixing 2 g of ferrihydrite with 15 mL of a 1 M NaOH solution containing $Pb(NO_3)_2$. The final concentration of Pb in the slurry was 13.3 mM Pb (0.52 μmol/m^2) and the final pH was 13.2 (±0.1). The mixture was equilibrated under constant stirring for 30 min, after which the high temperature transformation experiments (i.e., in situ and ex situ transformations, see below) were immediately started. Corresponding experiments with no Pb present were carried out (−Pb system) but with the ferrihydrite also equilibrated with 1 M NaOH for 30 min prior to initiation of the transformation reactions at high temperatures.

The crystallization of ferrihydrite was followed in situ using time-resolved synchrotron-based EDXRD.[23,24] The experiments were performed on beamline 16.4 of the Synchrotron Radiation Source, Daresbury Laboratory, UK. A detailed description of the experimental protocol can be found in refs 15 and 16. The transformation reactions were performed under isothermal conditions at temperatures between 160 and 240 °C using a Teflon-lined steel hydrothermal cell. The temperature range chosen reflects the limitations of beamtime access in order to use the EDXRD technique effectively. Diffraction patterns of the cells contents were collected at 1 min intervals and experiments were conducted for a maximum of 8.5 h depending on the temperature.

Transformation experiments were also conducted off-line, ex situ at 180 °C using similar Teflon-lined steel hydrothermal cells as in the online, in situ experiments. The pH of the −Pb and +Pb systems remained unchanged at pH 13.2 ± 0.1 both after the adsorption stage and during the transformation (both in situ and off-line transformations). The off-line reactions were quenched at specific times (i.e., 5, 10, 12, 17, 22, 32, 54, and 100 min) and the solid and liquid phases were immediately separated by centrifugation. The liquid phase was filtered through a 0.2 μm polycarbonate filter, acidified to pH 2 using a 3 M HNO_3 solution, and refrigerated at 4 °C prior to Pb analysis (see below). The solid phases were washed three times with deionized water and freeze-dried.

Desorption Experiments: The Speciation of Pb. Chemical extractions were performed to quantify the speciation of Pb during the ex-situ crystallization reactions. Specifically, the mass balance of Pb in the system: Pb in solution (Pb-SL), surface adsorbed Pb (Pb-SF), and incorporated Pb within the particles (Pb-INC) were determined via

$$(\text{Pb-T}) = (\text{Pb-SL}) + (\text{Pb-SF}) + (\text{Pb-INC})$$

where (Pb-T) is the total amount of Pb initially added into the system. The proportion of Pb-SL was determined from the amount of Pb in the filtered supernatant of the ex situ quenched samples. Second, a duplicate of each quenched ex situ experimental slurry (supernatant solution + solids) was titrated quickly to pH 2 using 3 M HNO_3 and equilibrated for 30 min with stirring. This led to the desorption of any Pb from the iron (oxyhydr)oxide surfaces. After the desorption, the resulting solid and liquid samples were separated. These desorption solutions contained two pools of Pb (a) in solution (Pb-SL) and surface adsorbed (Pb-SF). In all cases, the concentration of Pb was quantified by atomic absorption spectrometry (AAS) using a Varian AAS-10 spectrometer with the error being the standard deviation from the mean of three repeated measurements of two repeated off-line experiments. From the solution analyses, the surface bound lead (Pb-SF) was then calculated by subtracting the Pb-SL from the amount of Pb extracted at pH 2 for 30 min during the desorption. Finally, the incorporated Pb (Pb-INC) was determined from the difference between the total lead (Pb-T) and the sum of (Pb-SL + Pb-SF).

Off-Line Solid Characterization. The solid phases in the experiments (starting material, intermediate quenched samples and end products) were characterized by conventional X-ray powder diffraction (XRD, Philips PW1050 X-ray diffractometer, CuKα) using an internal silicon standard. Unit cell dimensions for the crystalline end products were calculated using the software Unitcell.[25] The freeze-dried samples were imaged using a field emission gun scanning electron microscope (FEG-SEM, LEO1530, 3 keV) and a FEG-transmission electron microscope (FEG-TEM, Phillips, CM200, 197 keV). The Brunauer−Emmett−Teller (BET) surface areas of the quenched, washed, and freeze-dried solid products were measured using a Gemini V2365 system (Micromeritics Instrument Corp.)

Results and Discussion

Online, in Situ Transformation and off-Line, Ex Situ Transformations. The time-resolved energy dispersive diffraction data (Figures 1 and 2) showed that in the presence of Pb (+Pb system) and absence of Pb (−Pb system) ferrihydrite crystallized to goethite and hematite via a two-stage process (see also Supporting Information, Figures 1 and 2). During the first stage, a relatively short induction period (360−745 s, Table 1) was followed by the growth of both goethite and hematite peaks until the goethite peaks reached a maximum intensity and began decreasing. At this point, the first stage of the transformation was complete (e.g., at 8 min, Figures 1b and 2b). At any given temperature, the ratio between goethite and hematite peak intensities during the first stage of the reaction in the −Pb system was notably

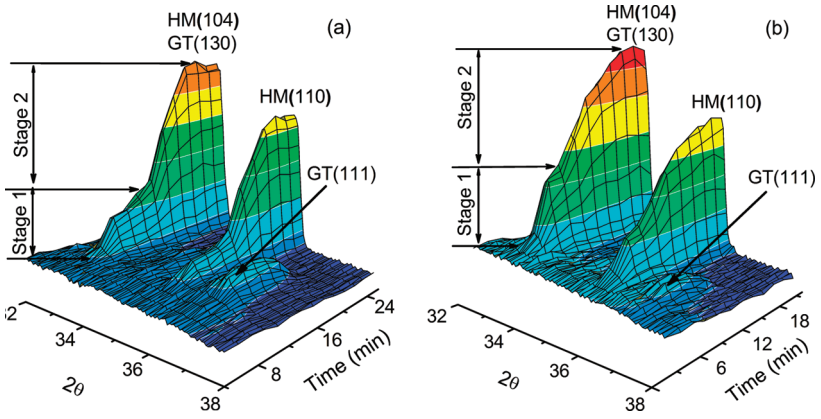

Figure 1. 3D time-resolved EDXRD plots representing the transformation of ferrihydrite to hematite at 240 °C for the −Pb (a) and +Pb systems (b). Note that the GT(110) peak is absent because this peak has a two theta of 21.24 which is off the scale of the figure.

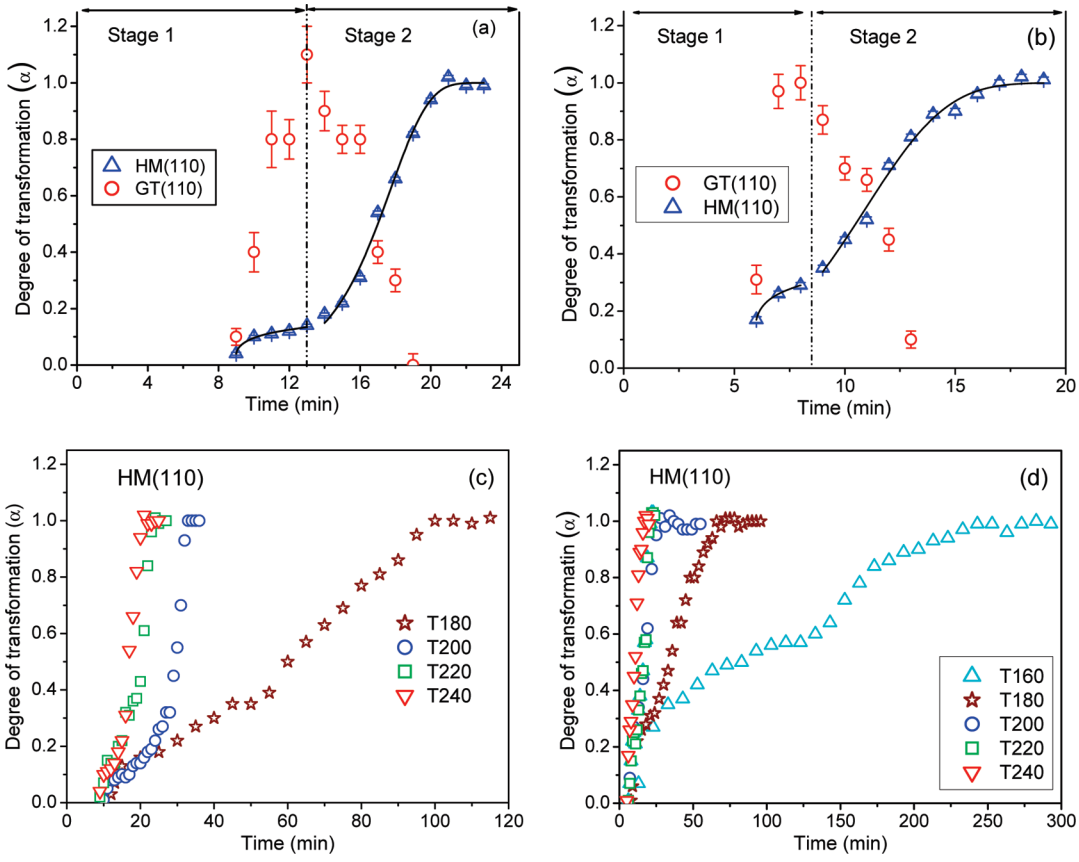

Figure 2. Degree of transformation for the goethite (GT, 110) peak growth and decay, and hematite (HM, 110) peak growth in the two stages (solid lines in (a) and (b) are the JMAK fits (see eq 1) for hematite growth) at 240 °C; (a) −Pb system and (b) +Pb systems; (c) degree of transformation for the HM (110) peak at different temperatures for the −Pb and (d) degree of transformation for the HM (110) peak at different temperatures for the +Pb system. Note the error bars in (c) and (d) are smaller than the symbols.

larger than in the +Pb system (Figure 1a,b, and Supporting Information, Figure S1a,c). During the second stage, hematite continued to form while the diffraction peaks for goethite decreased, leading to a final end product of pure hematite (e.g., end parts of Figures 1b and 2b). Although ferrihydrite was present at the beginning of all reactions, due to the low resolution of the EDXRD technique[26] and the poorly ordered nature of the starting ferrihydrite,[27] no diffraction peaks for ferrihydrite were observed. The evaluation of the data showed that in the +Pb system at all temperatures, the induction times (first time of appearance of a Bragg peak, see eq 1) were ∼20−30% shorter and the overall crystallization reactions were faster compared to the −Pb system (Figures 1 and 2, Table 1, and Supporting Information, Figures S1 and S2).

The end of the reactions was determined from the lack of change in the intensity of specific Bragg peaks (110 for HM). The EDXRD patterns were fitted using XFIT[28] to determine the peak areas of the (110) peaks for HM and GT as a function of time. To express the degree of reactions (α), the resulting peak areas were normalized to values between 0 and 1 with 0 or 1 representing the initial peak area of HM and GT respectively and 1/0 at the end of the reactions representing the maximum/minimum peak areas. The (110) diffraction

Table 1. Kinetic Parameters for the Growth of Hematite and Decay of Goethite in the +Pb and −Pb Systems for Both Stages[a]

	−Pb system						+Pb system					
	Stage 1 (m = 1)			Stage 2 (m = 2)			Stage 1 (m = 1)			Stage 2 (m = 2)		
T (°C)	t_o (s)	time interval (min)	hematite k (10^{-4} s^{-1})	time interval (min)	hematite k (10^{-5} s^{-1})	goethite k (10^{-5} s^{-1})	t_o (s)	time interval (min)	hematite k (10^{-4} s^{-1})	time interval (min)	hematite k (10^{-5} s^{-1})	goethite k (10^{-5} s^{-1})
160							745 (36)	14−48	12 (1)	91−249	19 (1)	
180	706 (14)	12−26	46 (4)	30−100	38 (2)		530 (10)	9−22	43 (3)	26−75	61 (2)	68 (4)
200	598 (6)	10−17	78 (7)	19−43	166 (20)	137 (11)	418 (5)	7−12	96 (9)	13−29	210 (4)	217 (18)
220	541 (5)	9−13	139 (27)	16−27	248 (49)	441 (58)	421 (4)	7−12	123 (13)	13−23	332 (13)	312 (25)
240	540 (3)	9−13	152 (13)	14−23	461 (29)	511 (84)	360 (2)	6−8	259 (36)	9−18	408 (41)	398 (42)
E_a (nucl)			9 (±2)						16 (±3)			
E_a (cryst)			41 (±7)		77(±14)				67(±8)		73(±11)	

[a] Standard errors for the activation energies and errors for t_o and k, in brackets, were calculated by regression. Shown also are the time intervals for each temperature for each stage respectively, as well as the m values used for each stage. Unit for activation energies is kJ/mol.

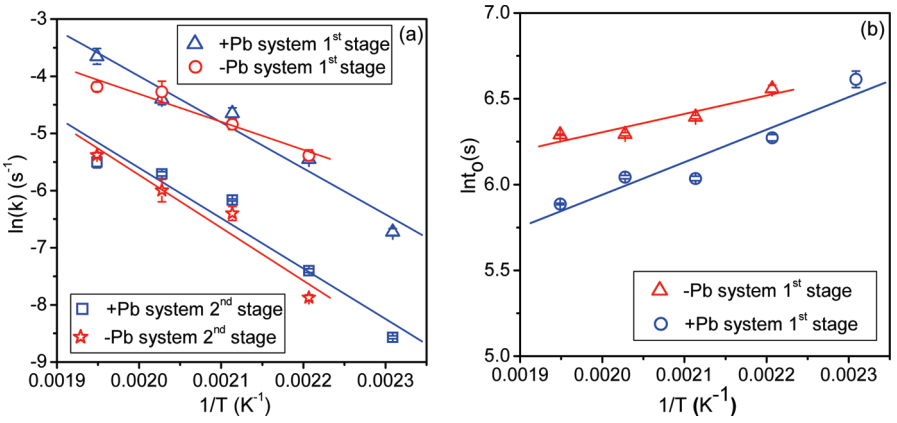

Figure 3. Arrhenius plots of (a) rates of hematite growth for both crystallization stages and (b) induction times for hematite in the 1st stage for both the +Pb and −Pb system (some error bars are smaller than the symbols).

peaks for HM (2θ of 35.64) and GT (2θ of 21.24) were chosen to avoid any possible overlaps and interferences with other peaks. The normalized values were subsequently fitted using the Johnson-Mehl-Avrami−Kolmogorov (JMAK) kinetic model[29−31] using the following equation:

$$\alpha = 1 - e^{-[k(t-t_o)]^m} \quad (1)$$

where α is the degree of the reaction, k (s^{-1}) is the rate constant, t (s) is time, t_o (s) is the induction time, and m is a constant related to the mechanism of the reaction. The obtained temperature-dependent rate constants and induction times were then used to calculate apparent activation energies for nucleation ($E_{a(nucl)}$) and crystallization ($E_{a(cryst)}$) using a similar approach and equivalent EDXRD data analysis procedures to ref 15.

Fitting the diffraction normalized peak areas using the JMAK kinetic model yielded values for induction times (t_o), rate constants (k), and exponential factors (m) for the crystallization of hematite in stages 1 and 2, and the decay of goethite in stage 2 (Table 1). In a first fitting step, the three main parameters from eq 1 (k, t_o, and m) were all regressed as free parameters via a nonlinear regression. For the m values, this fitting resulted in average m values of 0.8 ± 0.1 and 2.2 ± 0.5 for the first and the second stage of the +Pb system and average m values of 0.9 ± 0.3 and 2.4 ± 0.5 for the first stage and the second stage in the −Pb system, respectively. Previous studies of hematite and goethite crystallization from ferrihydrite suggested a first-order reaction equivalent to m = 1;[15,16] therefore, the data for the first stage of the reaction were refitted with m fixed to 1. For the second stage, both systems have average m values within an error of 2; therefore, the data for the second stage was refitted with m fixed at 2. Refitting of all data sets with m fixed to 1 and 2 for the first and second stages respectively but with k and t_o as regressed variables yielded reaction rates within the errors with the initial fitting, but for consistency and comparison with the literature, m of 1 and 2 were used. The kinetic data revealed that in both the +Pb and −Pb system with increasing temperature, t_o decreased while k increased. In addition, in the +Pb system the crystallization of hematite started on average ~20−30% earlier (see t_o in Table 1) than in the −Pb system. The correlation between induction times and reaction rates with temperatures suggests that the transformations were thermally activated processes. In each stage for both systems, the rates for hematite growth were similar (Table 1 and Figure 3) indicating that the presence of Pb had little influence on the reaction rates. In both systems, an m value of 1 for the first stage provided the best fit to the data, while for the second stage an average m value close to 2 was obtained, indicating that the transformation mechanisms remained consistent across the temperature range of this study. An m value of 1 for the first stage of hematite crystallization (from ferrihydrite) suggests a pseudo first order reaction, which is consistent with previous studies of ferrihydrite crystallization to hematite.[9,11,12,15,16] An m value of 2 for the second stage of crystallization suggests that goethite crystallized to hematite via a 2D growth mechanism.[32] The platelike morphology of the final hematite particles (Figure 4) also supports this conclusion. Finally, the rate constants and m values derived from the JMAK fitting of the

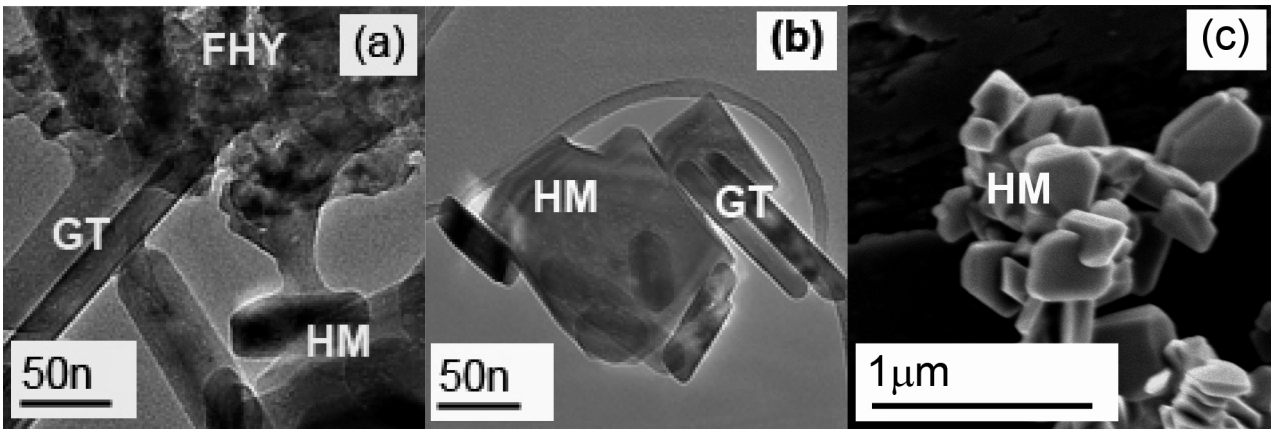

Figure 4. Photomicrographs of time-dependent changes in the solid phases (FHY = ferrihydrite, GT = goethite, and HM = hematite) from quenched off-line transformation experiments at 180 °C, in the +Pb system (a) after 12 min, (b) after 54 min, and (c) after 6.5 h.

time-resolved data were also confirmed by fitting the data using a double log approach[33] (Supporting Information, Figure S3, Table S1 and associated text) indicating the excellent correlation between these two fitting approaches.

It has been previously shown that adsorbed ions, including Pb^{2+}, can enhance the aggregation of colloids (e.g., hematite and kaolinite),[1,34] by neutralizing their surface charge and therefore reducing the electrostatic energy barrier between the particles and subsequently promoting aggregation. Calculation of surface coverage of Pb on the initial ferrihydrite yielded a maximum adsorption capacity of 1.5 mmol (see Supporting Information text for more details). The total concentration of Pb initially added into the +Pb system was 0.2 mmol or about 13% of the maximum adsorption capacity, indicating that the surface of the ferrihydrite was only partially neutralized by Pb adsorption. We suggest that this process favored the aggregation of the ferrihydrite particles which in turn enhanced the formation of hematite. This hypothesis is also supported by the substantially shorter induction times in the +Pb experiments (~20−30% shorter than in the −Pb system, Table 1). Although there are differences in terms of conditions of transformation when compared to previous studies (e.g., pH and temperature), the enhancement of hematite formation by the presence of Pb in the current study is comparable to previous results.[9]

Despite the large difference in induction times between the + Pb and −Pb systems, the derived $E_{a(nucl.)}$ values for hematite in both systems are similar (9 ± 2 and 16 ± 3 kJ/mol) although lower than previously reported values at equivalent conditions (25 kJ/mol[16]). This difference is likely a consequence of the higher solid/liquid ratio (133 g/L used in the present study compared to 100 g/L used for the work in ref 16) and the presence of Pb (see above). In addition, it was shown previously[35] that the rate of aggregation of colloids is linked to the concentration of particles in the suspension via

$$\frac{dN}{dt} = -k_a N^2 \qquad (2)$$

where N is the concentration of particles in suspension at time t, k_a ($k_a = \alpha_a \beta$) is the rate constant with α_a being a mass transport coefficient ($m^3\ s^{-1}$) and β the collision efficiency. From the above equation, it can be seen that if the concentration of particles increases the rate of aggregation of particles also increases. In the current study, both factors (i.e., the higher concentration of ferrihydrite and the presence of Pb) enhanced the aggregation of our starting ferrihydrite and thus this may have lowered the energy required to overcome the barrier for hematite nucleation.

The calculated $E_{a(cryst.)}$ for the two systems in both stages (Table 1) are within the ranges of activation energies previously reported for these reactions.[15,16] Furthermore various studies[16,18,36] have concluded that hematite crystallized from goethite via a water aided topotactic reaction that followed a 2D growth pathway. The activation energies derived from the current study on the crystallization of hematite from goethite (2nd stage, +Pb and −Pb system) are consistent with this mechanism.

SEM and TEM images (Figure 4) and XRD data (Supporting Information, Figure S4) of the quenched reaction products from the off-line transformation experiments at 180 °C in the +Pb system further verified the two-stage crystallization, with hematite as sole end product. The micrographs showed that after 12 min of reaction ferrihydrite, goethite, and hematite were all present (Figure 4a), while after 54 min only goethite and hematite were visible (Figure 4b). Finally, at the end of the reaction (6.5 h) hematite was the only phase present (Figure 4c, Supporting Information, Figure S3). Goethite was present as needlelike crystals of between 50 and 500 nm, while hematite was present as platy crystals about 100−500 nm in size. In order to evaluate the association of Pb with the various phases during the reaction, energy dispersive X-ray analyses (EDS) of the individual phases by TEM was used. The data (Figure 5) revealed that Pb was associated with the hematite and goethite phases throughout the transformation, indicating that the bulk concentration of Pb in each of these phases was >0.1 atomic% (detection limit of the EDS analysis).[37]

In contrast to the results in this work, previous studies that followed the crystallization of ferrihydrite at high pH concluded that goethite was the stable end product at pH ~13.[38] However, a recent study where poorly ordered schwertmannite ($Fe_8O_8(OH)_6SO_4$) was reacted at high pH (13.2), high temperatures (60−240 °C) and at a high solid to solution ratio (100 g of ferrihydrite/L solution) showed that above 150 °C the sole end product was also hematite, and that the reaction progressed also via a two-stage process with ferrihydrite and goethite as intermediates.[16] The authors[16] suggested that the formation of hematite in their system was due to (a) the presence of sulfate (from the dissolution of schwertmannite) and (b) the high temperature conditions. Other studies suggested that a high solid to solution ratio may also be the reason for hematite formation at high pH.[39]

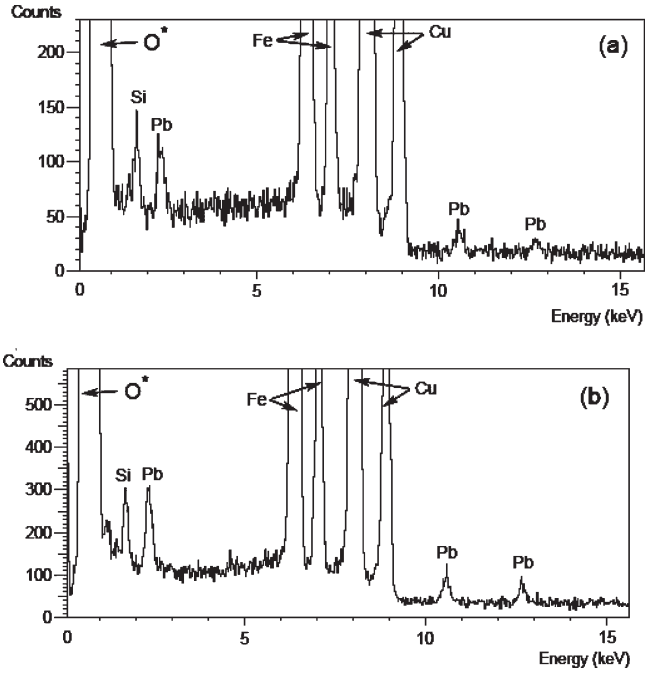

Figure 5. TEM−EDS spectra showing that Pb was associated with goethite (a) and hematite (b) during the transformation (the presence of Cu in the pattern is due to the TEM grid). *Some counts from Fe and Cu may be hidden within the main O peak.

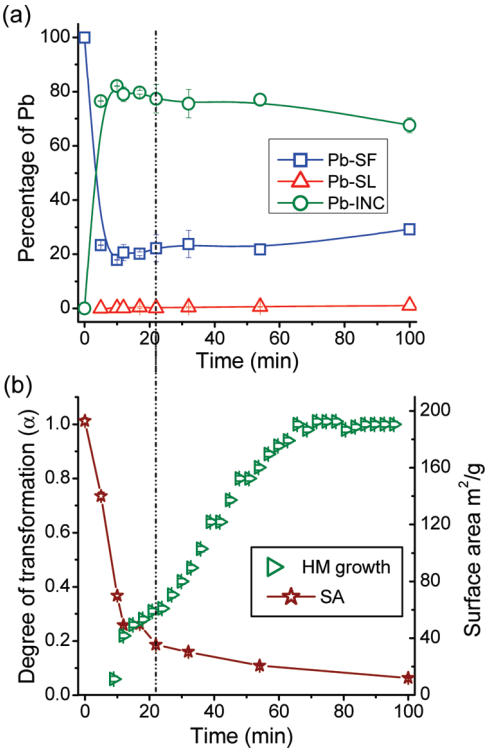

Figure 6. Partitioning of Pb during the transformation of ferrihydrite to hematite in the +Pb system (a) and the degree of transformation (α) from the EDXRD data for HM (same data as in Figure 2d and Supporting Information, Figure S1d) and the change in surface area (SA) of the solid fractions at 180 °C (b). Pb-SL = Pb in solution; Pb-SF = surface adsorbed Pb; Pb-INC = incorporated Pb within particles. Some of the error bars are smaller than the symbols. Vertical dotted line at 22 min delineates the first and second stage of crystallization.

Therefore, we conclude that the combination of an initial high solid to solution ratio (133 g of ferrihydrite/L solution) and high temperature (160−240 °C) conditions favored the formation of a pure hematite end product in the present study. In addition, fitting the goethite peak intensity decrease during the second stage yielded rate constants similar to those for the growth of hematite (Table 1), indicating a direct transformation of goethite to hematite, analogous to that reported in ref 16.

Speciation of Pb during the Transformation and Interaction of Pb with Iron (Oxyhydr)oxides. The solution chemistry data for the +Pb system (Figure 6) as well as the EDS analyses (Figure 5) revealed that Pb was associated with the solid phases (ferrihydrite, goethite, and hematite) throughout the crystallization process. In the starting ferrihydrite (0 min, Figure 6), Pb was fully adsorbed (~100%) to the ferrihydrite surface. However, soon after the crystallization reaction was initiated (after 12 min), a significant increase in Pb-INC (from 0 to ~80%) and a corresponding decrease in Pb-SF (100% to ~20%) occurred. In conjunction with this, a significant decrease in the surface area of the solid phases (from 193 down to 49 m^2/g) was observed. Most of this change in surface area and Pb speciation occurs before any XRD peaks for hematite were detected, indicating that the Pb was incorporated into the ferrihydrite aggregates before the crystallization process began. The EDXRD data (Figure 6b, triangles) reveals that hematite formation was initiated after approximately 9 min, and after 12 min about 20% of hematite had crystallized. From 12 to 22 min, an additional, but more gradual rise in the amount of hematite (from 20 to about 30%) was observed. Continuing nucleation and growth of hematite (and goethite, and the full consumption of ferrihydrite, Supporting Information, Figure S4) coincided with a slower decline in the surface areas of the solids (from 49 down to 35 m^2/g) during this later part of stage 1 (12−22 min, Figure 6). However, during this latter part of stage 1, the Pb-INC, the Pb-SF, and the Pb-SL remained unchanged.

During the second crystallization stage (after the 22nd min), hematite crystallized steadily from goethite until the transformation was completed and hematite was the sole solid phase present. Pb-INC decreased from 77 to 67% ,and this was accompanied by a corresponding small increase in the Pb-SF and Pb-SL (22−29% and 0.4−3.2%, respectively). Again the surface areas of the solid phases (goethite and hematite) further decreased (from 35 m^2/g at the beginning of this stage to 12 m^2/g at the end of the reaction), and this corresponded to the final disappearance of goethite and predominance of hematite at the end of stage 2 (Figure 6).

The data presented above revealed that the largest proportion (~80%) of Pb in the system became incorporated into the solid phases very close to the beginning of the reactions but clearly prior to the initiation of the first crystallization stage (Figure 6), and thus the mechanism of Pb incorporation was controlled by a process, which occurred prior to hematite/goethite crystallization. Fischer and Schwertmann suggested that hematite formation from ferrihydrite proceeds first via the aggregation of the poorly order ferrihydrite nanoparticle followed by their crystallization and that the crystallization involves internal rearrangements within the hydrated ferrihydrite nanoparticle aggregates.[12] The data from this study indicate that the incorporation of Pb into the iron phases occurs fast and is controlled by this aggregation process, which occurs prior to the initiation of hematite crystallization. We suggest that when the ferrihydrite

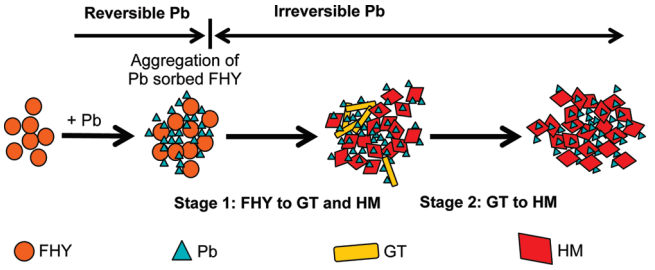

Figure 7. A schematic of the processes governing the fate of Pb during the crystallization reactions described in this study.

nanoparticles aggregate, the adsorbed Pb on the surface will be retained at the interface between the ferrihydrite nanoparticles, and consequently, during the crystallization, the Pb will become irreversibly incorporated within the interstices of the hematite particles (Figure 7). This is supported by the rapid decrease in SA during the initial induction period. The ionic radius of Pb^{2+} (1.19 Å) is about double that of Fe^{3+} (0.643 Å), and thus it is unlikely that Pb would replace Fe^{3+} in the structure of newly formed iron (oxyhydr)oxides. However, the high proportion of Pb in the hematite or goethite particles (large Pb-INC pool) could stem from its incorporation into structural defects caused by the trapping of the Pb within the crystals of hematite and/or goethite during the aggregation/growth process of the first stage of crystallization. Goethite was formed during this first stage of crystallization, but it starts to form at the same time as hematite. However, goethite constitutes only a small proportion of the total amount of crystalline material (comparing the ratio of goethite and hematite intensity in Figure 1a,b, and Supporting Information, Figure S1a,c) at the end of the first phase. Therefore, we conclude that the aggregation of ferrihydrite prior to hematite formation is the dominant process controlling Pb incorporation.

For the transformation of goethite to hematite in the second stage, the Pb sorbed onto the surface of goethite as well as any Pb present in the structural defects of goethite will become incorporated within the hematite structure upon transformation. Goethite is known to have a higher capacity of incorporating foreign cations into its structure than hematite,[1,40] and therefore any transformation will result in the decline in the Pb-INC pool during this stage of the reaction. Our data confirms this trend as the Pb-INC pool decreases from 77 to 67% during this stage (Figure 6). Evaluating the potential effects of the incorporated Pb on the unit cell size of the end product hematite revealed that the *a* and *c* parameters of the hematite were barely affected (expanded by 0.04 and 0.01%, respectively, Supporting Information, Table S2), further supporting the hypothesis that Pb is not directly substituting for Fe in the structure of hematite. Martinez et al.[22] suggested that the release of Pb into solution during hematite crystallization may be due to a reduction in sorption sites which results in a lower retention capacity of the solid. The results from the present study show that as hematite crystallizes, during the second stage, the amount of surface bound Pb (Pb-SF) actually increases and that the increase in labile Pb (Pb-SL and Pb-SF) is due to Pb being expelled from the defects in the hematite structure. The crystallization of hematite (specifically at high temperatures) will reduce the number of defects in the structure, therefore reducing the number of structural defect sites in which the Pb can be accommodated.[40] The expelled Pb will subsequently either be adsorbed to the particle surfaces or released into solution.

Previous studies that followed the aging of ferrihydrite with adsorbed or coprecipitated Pb at low temperatures (room to 70 °C)[8,9,20−22] showed that (a) the end products were usually non-monomineralic, (b) the largest proportion of the total Pb was released back into solution during ferrihydrite crystallization, and (c) only 10% of the total Pb became incorporated into the structure of the end products. The calculated Pb mol % relative to Fe (Pb/(Fe + Pb)*100) indicate that the hematite end product contains ∼0.76% Pb. This value is lower than the maximum Pb^{2+} which can substitute in some iron (oxyhydr)oxide phases, for example, up to 2.8% in goethite.[41] However, compared to other studies that produced hematite and goethite by aging ferrihydrite with adsorbed or coprecipitated Pb,[9,20,22] the proportion of Pb incorporated (up to 70%) is much higher and the speed of uptake much more rapid (< 12 min at 180 °C). This clearly demonstrates that the chemical and physical conditions in these reactions were optimized for Pb incorporation into the hematite end product. We suggest that the high solid/solution ratio and the rapid rate of crystallization, facilitated by the high pH and temperature, are the main factors controlling this enhanced uptake process. First, the high temperature and the solid/solution ratio caused the rapid aggregation of the ferrihydrite nanoparticle (see ref 1 and references therein and ref 35), and this helped trap the adsorbed Pb within the aggregates. Second, the rapid crystallization kinetics for hematite (∼70 min at 180 °C) is faster than the release of Pb from the particles and allows the Pb to be retained within the structure.

Conclusion

The present study is one of the first to have shown that at high pH and high temperatures goethite is an intermediate phase in the transformation of ferrihydrite to hematite and that large amounts (up to 70%) of the Pb in the system can become irreversibly incorporated within the hematite particles, while only a small proportion of the total Pb is released back into solution during the crystallization. Our data indicate that Pb is rapidly sequestered prior to the start of hematite crystallization, and this process is controlled by the aggregation of the ferrihydrite nanoparticles, which trap the Pb ions within the aggregates. This detailed information on the mechanism and kinetics of Pb uptake and iron (oxyhydr)oxide crystallization was obtained due to the unique experimental and analytical approach utilized within the research, which combines in situ diffraction, chemical extractions, and surface area analyses. The results of this study show how the incorporation of Pb can be enhanced by the chemical and physical conditions of iron (oxyhydr)oxide crystallization. These findings are particularly relevant to the long-term geological disposal/storage of intermediate-level radioactive waste and Pb transport associated with iron-rich colloidal particles in natural environments.

Acknowledgment. This research was funded by a Dorothy Hodgkin Postgraduate Award (H.P.V.) and UK CCRLC awards for beamtime (47113 and 50115) to L.G.B. We acknowledge David Taylor and Tony Bell from station 16.4, Daresbury Laboratory, UK, and Juan Diego Rodriguez-Blanco and Gabriella Kakonyi from the University of Leeds for their help with collecting the EDXRD data; Steeve Bonneville from the University of Leeds is acknowledged

for his help with the TEM imaging. We would like to thank the associate editor and three anonymous reviewers for their comments, which helped to improve the quality of the manuscript.

Supporting Information Available: Figure S1: time-resolved EDXRD patterns and degree of reaction data from the in situ transformation experiments at 180 °C for the +Pb and −Pb systems; Figure S2: details of Figure 2c,d (main document) for the −Pb and +Pb systems; Figure S3: double log plots and associated text with explanations; Figure S4: XRD patterns from an off-line transformation experiments at 180 °C with spectra between 30 min and 6.5 h;

Table S1: Kinetic parameters based on the double log approach (Figure S3); Table S2: calculated unit cell parameters for the +Pb and −Pb hematite end products. Finally, some text related to the unit cell and surface coverage calculation is presented. This information is available free of charge via the Internet at http://pubs.acs.org/.

References

(1) Cornell, R. M.; Schwertmann, U. *The Iron Oxides: Structure, Properties, Reactions, Occurrences and Uses*; Wiley-VCH: Weinheim, 2003; p 703.

(2) Loan, M.; Parkinson, G.; Newman, M.; Farrow, J. Iron oxyhydroxide crystallization in a hydrometallurgical residue. *Cryst. Growth Des.* **2002**, *235* (1−4), 482–488.

(3) Hering, J. G.; Chen, P. Y.; Wilkie, J. A.; Elimelech, M.; Liang, S. Arsenic removal by ferric chloride. *J. Am. Water Work Assoc.* **1996**, *88* (4), 155–167.

(4) Scherer, M. M.; Richter, S.; Valentine, R. L.; Alvarez, P. J. J. Chemistry and microbiology of permeable reactive barriers for *in situ* groundwater clean up. *Crit. Rev. Environ. Sci. Technol.* **2000**, *30* (3), 363–411.

(5) Hassellov, M.; von der Kammer, F. Iron oxides as geochemical nanovectors for metal transport in soil-river systems. *Elements* **2008**, *4* (6), 401–406.

(6) Benjamin, M. M.; Sletten, R. S.; Bailey, R. P.; Bennett, T. Sorption and filtration of metals using iron-oxide-coated sand. *Water Res.* **1996**, *30* (11), 2609–2620.

(7) Lundtorp, K.; Jensen, D. L.; Sorensen, M. A.; Christensen, T. H.; Mogensen, E. P. B. Treatment of waste incinerator air-pollution-control residues with $FeSO_4$: Concept and product characterisation. *Waste Manage. Res.* **2002**, *20* (1), 69–79.

(8) Martinez, C. E.; McBride, M. B. Coprecipitates of Cd, Cu, Pb and Zn in iron oxides: Solid phase transformation and metal solubility after aging and thermal treatment. *Clays Clay Miner.* **1998**, *46* (5), 537–545.

(9) Ford, R. G.; Kemner, K. M.; Bertsch, P. M. Influence of sorbate-sorbent interactions on the crystallization kinetics of nickel- and lead-ferrihydrite coprecipitates. *Geochim. Cosmochim. Acta* **1999**, *63* (1), 39–48.

(10) McKinley, I. G. The management of long lived nuclear waste. *Energy Policy* **1992**, *20* (7), 683–692.

(11) Schwertmann, U.; Murad, E. Effect of pH on the formation of goethite and hematite from ferrihydrite. *Clays Clay Miner.* **1983**, *31* (4), 277–284.

(12) Fischer, W. R.; Schwertmann, U. Formation of hematite from amorphous iron(III) hydroxide. *Clays Clay Miner.* **1975**, *23* (1), 33–37.

(13) Loan, M.; Newman, O. M. G.; Farrow, J. B.; Parkinson, G. M. Continuous reactive crystallization of nanoscale six-line ferrihydrite. *Cryst. Growth Des.* **2006**, *6* (1), 79–86.

(14) Loan, M.; Newman, O. G. M.; Farrow, J. B.; Parkinson, G. M. Effect of rate of crystallization on the continuous reactive crystallization of nanoscale 6-line ferrihydrite. *Cryst. Growth Des.* **2008**, *8* (4), 1384–1389.

(15) Shaw, S.; Pepper, S. E.; Bryan, N. D.; Livens, F. R. The kinetics and mechanisms of goethite and hematite crystallization under alkaline conditions, and in the presence of phosphate. *Am. Mineral.* **2005**, *90* (11−12), 1852–1860.

(16) Davidson, L. E.; Shaw, S.; Benning, L. G. The kinetics and mechanisms of schwertmannite transformation to goethite and hematite under alkaline conditions. *Am. Mineral.* **2008**, *93* (8−9), 1326–1337.

(17) Schwertmann, U.; Stanjek, H.; Becher, H. H. Long-term in vitro transformation of 2-line ferrihydrite to goethite/hematite at 4, 10, 15 and 25 degrees C. *Clay Miner.* **2004**, *39* (4), 433–438.

(18) Murray, J.; Kirwan, L.; Loan, M.; Hodnett, B. K. In-situ synchrotron diffraction study of the hydrothermal transformation of goethite to hematite in sodium aluminate solutions. *Hydrometallurgy* **2009**, *95* (3−4), 239–246.

(19) Schwertmann, U.; Friedl, J.; Stanjek, H. From Fe(III) ions to ferrihydrite and then to hematite. *J. Colloid Interface Sci.* **1999**, *209* (1), 215–223.

(20) Ford, R. G.; Bertsch, P. M.; Farley, K. J. Changes in transition and heavy metal partitioning during hydrous iron oxide aging. *Environ. Sci. Technol.* **1997**, *31* (7), 2028–2033.

(21) Martinez, C. E.; McBride, M. B. Solubility of Cd^{2+}, Cu^{2+}, Pb^{2+}, and Zn^{2+} monitored in aged coprecipitates with amorphous iron hydroxides. *Environ. Sci. Technol.* **1998**, *32* (6), 743–748.

(22) Martinez, C. E.; Sauve, S.; Jacobson, A.; McBride, M. B. Thermally induced release of adsorbed Pb upon aging ferrihydrite and soil oxides. *Environ. Sci. Technol.* **1999**, *33* (12), 2016–2020.

(23) Shaw, S.; Clark, S. M.; Henderson, C. M. B. Hydrothermal formation of the calcium silicate hydrates, tobermorite ($Ca_5Si_6O_{16}(OH)_2 \cdot 4H_2O$) and Xonotlite ($Ca_6Si_6O_{17}(OH)_2$): an in situ synchrotron study. *Chem. Geol.* **2000**, *167* (1−2), 129–140.

(24) Croker, D.; Loan, M.; Hodnett, B. K. Kinetics and mechanisms of the hydrothermal crystallization of calcium titanate species. *Cryst. Growth Des.* **2009**, *9* (5), 2207–2213.

(25) Holland, T. J. B.; Redfern, S. A. T. Unit cell refinement from powder diffraction data: The use of regression diagnostics. *Mineral. Mag.* **1997**, *61* (1), 65–77.

(26) Parise, J. B. Synchrotron studies of phase transformations. In *Transformation Processes in Minerals*; Redfern, S. A.T., Carpenter, M. A., Eds; Reviews in Mineralogy and Geochemistry, Vol. 39; Mineralogical Society of America: Washington, DC, 2000; pp 285−318.

(27) Janney, D. E.; Cowley, J. M.; Buseck, P. R. Structure of synthetic 2-line ferrihydrite by electron nanodiffraction. *Am. Mineral.* **2000**, *85* (9), 1180–1187.

(28) Cheary, R. W.; Coelho, A. A fundamental parameters approach to X-ray line-profile fitting. *J. Appl. Crystallogr.* **1992**, *25*, 109–121.

(29) Avrami, M. Kinetics of phase change, I. *J. Chem. Phys.* **1939**, *7*, 1103–1112.

(30) Avrami, M. Kinetics of phase change, II. *J. Chem. Phys.* **1939**, *8*, 212–224.

(31) Johnson, P. F.; Mehl, R. F. *Reaction Kinetics in Processes of Nucleation and Growth*; American Institute of Mining Engineering: Littleton, CO, 1939; Technical Publication No. 1089; pp 1−27.

(32) Hulbert, S. F. Models of solid-state reactions in powder compacts: A review. *J. Brit. Ceram. Soc.* **1969**, *6*, 11–20.

(33) Putnis, A. *An Introduction to Mineral Sciences*; Cambridge University Press: Cambridge, UK1992; p 480.

(34) Heidmann, I.; Christl, I.; Kretzschmar, R. Aggregation kinetics of kaolinite-fulvic acid colloids as affected by the sorption of Cu and Pb. *Environ. Sci. Technol.* **2005**, *39* (3), 807–813.

(35) Stumm, W.; Morgan, J. J. *Aquatic Chemistry: Chemical Equilibria and Rates in Natural Waters*; John Wiley and Sons, Inc.: New York, 1996; p 1022.

(36) Naono, H.; Nakai, K.; Sueyoshi, T.; Yagi, H. Porous texture in hematite derived from goethite - mechanism of thermal-decomposition of goethite. *J. Colloid Interface Sci.* **1987**, *120* (2), 439–450.

(37) Williams, D. B.; Carter, C. B. *Transmission Electron Microscopy: A Textbook for Materials Science*; Springer: New York, 1996; p 729.

(38) Cornell, R. M.; Giovanoli, R. Effect of solution conditions on the proportion and morphology of goethite formed from ferrihydrite. *Clays Clay Miner.* **1985**, *33* (5), 424–432.

(39) Schwertmann, U.; Fischer, W. R. Zur Bildung von α-FeOOH und α-Fe_2O_3 aus amorphem Eisen(III)-hydroxid. III. *Z. Anorg. Allg. Chem.* **1966**, *346* (3−4), 137–142.

(40) Brown, G. E.; Henrich, V. E.; Casey, W. H.; Clark, D. L.; Eggleston, C.; Felmy, A.; Goodman, D. W.; Gratzel, M.; Maciel, G.; McCarthy, M. I.; Nealson, K. H.; Sverjensky, D. A.; Toney, M. F.; Zachara, J. M. Metal oxide surfaces and their interactions with aqueous solutions and microbial organisms. *Chem. Rev.* **1999**, *99* (1), 77–174.

(41) Kaur, N.; Grafe, M.; Singh, B.; Kennedy, B. Simultaneous incorporation of Cr, Zn, Cd and Pb in the goethite structure. *Clays Clay Miner.* **2009**, *57* (2), 234–250.